Archival Report

Biological Psychiatry: GOS

Predicting Mental and Neurological Illnesses Based on Cerebellar Normative Features

Milin Kim, Nitin Sharma, Esten H. Leonardsen, Saige Rutherford, Geir Selbæk, Karin Persson, Nils Eiel Steen, Olav B. Smeland, Torill Ueland, Geneviève Richard, Aikaterina Manoli, Sofie L. Valk, Dag Alnæs, Christian F. Beckman, Andre F. Marquand, Ole A. Andreassen, Lars T. Westlye, Thomas Wolfers, and Torgeir Moberget, for the Alzheimer's Disease Neuroimaging Initiative

ABSTRACT

BACKGROUND: Mental and neurological conditions have been linked to structural brain variations. However, aside from dementia, the value of brain structural characteristics derived from brain scans for prediction is relatively low. One reason for this limitation is the clinical and biological heterogeneity inherent to such conditions. Recent studies have implicated aberrations in the cerebellum, a relatively understudied brain region, in these clinical conditions.

METHODS: Here, we used machine learning to test the value of individual deviations from normative cerebellar development across the lifespan (based on trained data from >27,000 participants) for prediction of autism spectrum disorder (ASD) (n = 317), bipolar disorder (n = 238), schizophrenia (SZ) (n = 195), mild cognitive impairment (n = 122), and Alzheimer's disease (n = 116); individuals without diagnoses were matched to the clinical cohorts. We applied several atlases and derived median, variance, and percentages of extreme deviations within each region of interest.

RESULTS: The results show that lobular and voxelwise cerebellar data can be used to discriminate reference samples from individuals with ASD and SZ with moderate accuracy (the area under the receiver operating characteristic curves ranged from 0.56 to 0.65). Contributions to these predictive models originated from both anterior and posterior regions of the cerebellum.

CONCLUSIONS: Our study highlights the utility of cerebellar normative modeling in predicting ASD and SZ, aided by 4 cerebellar atlases that enhanced the interpretability of the findings.

https://doi.org/10.1016/j.bpsgos.2025.100541

Clinical heterogeneity and complex pathobiological mechanisms impede the discovery of reliable biomarkers for many neurological and especially psychiatric disorders, thereby complicating precise clinical decision making and treatments. Over the last 2 decades, there has been a trend in the development of neuroimaging-based tools and machine learning for prognosis and diagnosis of psychiatric disorders (1,2) and neurological illnesses (3). Neuroimaging-based prediction studies of autism spectrum disorder (ASD), bipolar disorder (BD), and schizophrenia (SZ) have reported a wide range of accuracies, underscoring the limitations associated with small samples, including poor generalization performance (4,5). Notably, prediction studies on dementia have shown greater promise for clinical usage in both Alzheimer's disease (AD) (3) and mild cognitive impairment (MCI).

Notably, most of these prediction studies (4–6) have focused on cerebral features, perhaps reflecting a cortico-centric bias in the literature (7). Nonetheless, disruptions in the cerebellum have been hypothesized to contribute to early cognitive disturbances (8) and various clinical conditions, such as childhood psychiatric symptoms (9), AD (10), SZ (11), and ASD (12–14). Using a normative modeling approach, we recently demonstrated significant deviations from normal cerebellar developmental across the lifespan in individuals with mental and neurodegenerative illnesses including SZ and AD (15). The deviation refers to instances where an individual falls outside the typical range. However, recent literature indicates that there are no significant differences in the cerebellum in ASD (16), a condition characterized by repetitive patterns in behaviors, restricted interests, and difficulties in social interaction and communication (17). This may be attributed to the presence of both positive and negative deviations in cerebellar characteristics (15). In contrast, several studies (11,18) of SZ indicate a reduction in cerebellar volume, particularly in regions associated with perception, language comprehension, and cognitive functions. Patient studies have shown that abnormalities in the cerebellum can exert a significant influence on motor, cognitive, and emotional functions (19–21); however, there has been little exploration of the role of the cerebellum in predicting and classifying mental and neurological illnesses. While these individual-level deviations revealed substantial cerebellar heterogeneity among individuals with the same

© 2025 THE AUTHORS. Published by Elsevier Inc on behalf of the Society of Biological Psychiatry. This is an open access article under the CC BY license (http://creativecommons.org/licenses/by/4.0/).

ISSN: 2667-1743

disorder, the value of these cerebellar features with respect to classifying these disorders remains uncertain.

In this study, we addressed this gap by performing a set of predictions of ASD, MCI, AD, BD, and SZ using magnetic resonance imaging (MRI)–based cerebellar features and cross-validated machine learning classifiers. We applied lobular and voxelwise normative models (15) and aggregated the median, variance, and percentage of extreme deviations across atlases (22,23). The features, specifically the percentage of extreme deviation, median, and variance for each of the different cerebellar atlas regions, illuminate the model performance in terms of prediction of the disorders and diseases, given different parcellations and features. Finally, for models that were able to meaningfully differentiate between patients and healthy control participants, we identified the cerebellar regions that contributed most to the prediction.

METHODS AND MATERIALS

Sample

The study sample consisted of individuals from the cerebellar lifespan normative model (15), where individuals without a diagnosis were split into a training set (n = 27,117; 54% female), a test set (n = 26,985; 53% females), and a clinical set (n = 1757; 30% females) (Figure 1A and Table S2). Individuals without diagnoses were matched to the clinical datasets of patients with AD, ASD, BD, MCI, and SZ (Table 1) using nearest-neighbor matching based on exact matches of sex and scanning site with age as implemented in *MatchIt* (24). The clinical datasets were obtained from the ABIDE I and II (Autism Brain Imaging Data Exchange I and II), ADNI (Alzheimer's Disease Neuroimaging Initiative), AIBL (The Australian Imaging, Biomarkers and Lifestyle Flagship Study), DEMGEN (Norwegian Dementia Genetics Network), and TOP (Thematically Organized Psychosis) cohorts. Information about each cohort and studies can be found in the corresponding publications (Table S1). If participants were scanned at several time points, only baseline scans were chosen for this study. Individuals who withdrew from the studies or lacked essential demographic information and T1-weighted MRI data were excluded from the analyses.

Lobular-Level Processing

The T1-weighted images were skull stripped using the FreeSurfer version 5.3 auto-recon pipeline (25) and reoriented to the standard FSL orientation using the *fslreorient2std* (26). Linear registration was performed using *flirt* (27), which utilized linear interpolation (with 6 degrees of freedom) and the default 1 mm FSL template (version 6.0). The borders were cropped at coordinates (6:173, 2:214, 0:160) to minimize their size without removing brain tissue. Finally, the voxel intensity values of all brain images were normalized to the range of (0, 1), adjusting the intensity values of each voxel to a standardized scale.

To segment the cerebellum, we utilized the Automatic Cerebellum Anatomical Parcellation Using U-Net with Locally Constrained Optimization (ACAPULCO) algorithm (28), a part of the Enhancing Neuro Imaging Genetics through Meta Analysis (ENIGMA) Cerebellum Volumetric Pipeline, which is a cerebellum parcellation algorithm based on convolutional neural networks. This algorithm delivers fast and precise quantitative in vivo regional assessment of the cerebellum. As part of the algorithm, the images were corrected for inhomogeneity by the N4 correction method (29) and registered to the 1-mm isotropic ICBM 2009c template in Montreal Neurological Institute (MNI) space using the Advanced Normalization Tools registration suite (30). The ACAPULCO algorithm is based on 15 expert manual delineations of an adult cohort (31). It achieves per-voxel labeling and uses postprocessing of the parcellation to correct for mislabeling and accurate segmentation. ACAPULCO segments the cerebellum into 28 cerebellar lobules and computes the volume (mm^3) for each lobule. These regions include bilateral lobules I–VI; crus I and II; lobules VIIB, VIIIA, VIIIB, and IX–X; vermis VI, VII, VIII, IX, and X; and the corpus medullare. To ensure data quality, participants with extreme outliers (2.698 SD above or below the mean) (32) in more than 2 lobules based on automated quality control measures were excluded. We set the threshold at 2 lobules because the differences between 1 and 2 lobules were not significant (see Supplemental Methods for detailed information on quality control).

Voxel-Level Processing

We used Spatially Unbiased Infratentorial Toolbox (SUIT) version 3.4 (33) to segment cerebellar gray and white matter voxel-based morphometry maps. SUIT leverages the outputs from ACAPULCO, an MNI-aligned T1 image (33,34), and an average mask derived from a randomly selected group of 300 individuals without a diagnosis. After segmentation, the gray matter maps were standardized for comparison by aligning them to SUIT space through Jacobian modulation, ensuring that each voxel reflected its proportional alignment to the original volume.

Normative Modeling

Normative modeling (35), similar to pediatric growth charts, addresses the limitation of case-control studies by mapping developmental and aging trajectories across the lifespan, thereby preserving individual-level inference in reference to large populations (36–38). Widely applied in clinical research (38–43), it helps detect extreme deviations in individuals. Here, we used this approach to normalize clinical groups against the population reference, accounting for age, sex, and site effects. We used a publicly available cerebellar normative model based on >27,000 individuals without diagnoses (15). The cerebellar normative model was developed using a large reference sample that spans ages 3 to 85 years. This broad age range allows us to map individual deviations from established norms within clinical cohorts, including young participants. The use of this extensive reference sample provides a basis for normalization and confound removal with respect to age, sex, and site. This normative model includes cerebellar lobules and voxelwise intensities, which differ across tissues (e.g., gray matter, white matter, cerebrospinal fluid) based on their proton density and relaxation properties, while adjusting for sex, age, and scanning site (Figure 1B).

To analyze the data, we utilized Bayesian linear regression with the likelihood warping method (44), incorporating the sinarcsinsh transformation (45,46), to handle nonlinear basis functions and non-Gaussian predictive distributions for large

A Dataset

Sample

Clinical Sets: Alzheimer's Disease
Autism Spectrum Disorder, Bipolar Disorder,
Mild Cognitive Impairment, Schizophrenia

Neurotypical: Matched to Clinical Sets

Input

Lobule

Voxel-wise

B Normative Model

Lobular / Voxel-wise Model

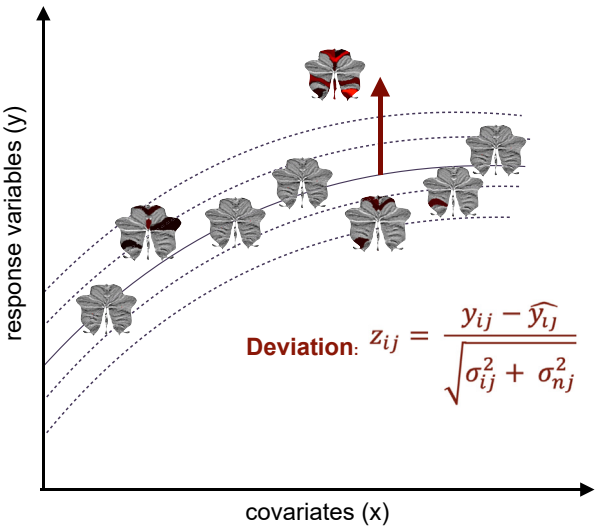

C Features and Models

Deviation Scores (Z-score)

Lobule Z-Score

Voxel-wise Z-Score

Cerebellum Atlases (ROIs as features)

Lobule (28)

Anatomical (28)

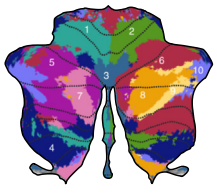

Task-based (10)

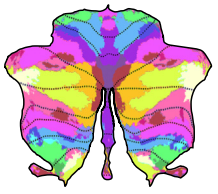

Hierarchical (32)

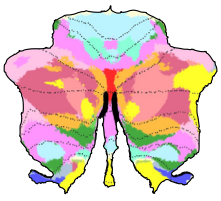

Resting-state (17)

Models

Volume (mm^3)

median,variance,
percentage of extreme positive deviation,
percentage of extreme negative deviation

datasets (45). Scanning site was accounted for as a fixed effect (47,48). The normative model provides point estimates and evaluation metrics such as explained variance, mean squared log loss, skew, and kurtosis (46). These evaluation metrics were calculated in the test set, which did not include clinical cohorts. Extreme deviations were defined as $|z| > 1.96$, corresponding to the most extreme 5% of cases in both directions in the reference cohort.

Feature Engineering

First, lobular normative models were used to derive deviation scores of volume for the 28 cerebellar lobules (Table S3). Second, voxelwise normative models were utilized to map deviation profiles of gray matter onto existing atlases (see Supplemental Methods for statistics and reproducibility). Four existing atlases were selected: 28 regions of interest (ROIs) from cerebellar anatomical atlas, 10 ROIs from a multidomain task battery (23), 32 ROIs from a hierarchical atlas (49), and 17 ROIs from resting-state connectivity (22,50) (see Atlases in Supplemental Methods and Figure S1 for labels). For each ROI delineated by these atlases, we computed 3 key statistics: the median, variance, and percentage of extreme deviations (Figure 1C). To quantify the percentage of extremes in deviation, we also calculated the proportion of voxelwise deviations that exceeded the established threshold of $|z| > 1.96$, denoting both extreme positive and negative deviations. This proportion was determined by dividing the count of such extreme deviations by the total voxel count within the corresponding ROI. Variance has previously been used to examine the structural heterogeneity among patients with SZ (51,52). Unlike percentage of extreme deviation ($|z| > 1.96$), which has been used in past normative studies (38,42,53), variance assesses the dispersion within the region, capturing the regionally heterogeneous spread within patients.

Model Training and Evaluation

Machine learning models using logistic regression (LR) were used to build prediction models (Figure 1D). The LR model was trained on the provided dataset, utilizing a logistic function to optimize weights to best fit the data. In addition, results from the random forest (RF) algorithm from the scikit-learn library version 1.2.2 (54) and the eXtreme Gradient Boosting (XGBoost) library version 1.7.3 (55) can be found in Figure S4. RF is a nonparametric supervised learning method that addresses overfitting by combining decision trees into a single outcome, effectively balancing the bias-variance trade-off. XGBoost is an open-source library to implement advanced gradient boosting algorithms (55).

Features were engineered across 4 atlases as well as for the different cerebellar lobules, serving as input to the LR algorithm, with diagnoses with respect to healthy individuals and clinical groups, such as ASD, BD, SZ, MCI, and AD, as labels. We utilized LR to assess predictive performance, using deviations from normative models, specifically their median, variance, and percentage of extreme deviations, derived from existing atlases superimposed onto voxelwise cerebellar maps. To evaluate the model's performance in the test set, we conducted a stratified 5-fold cross-validation and used the area under the receiver operating characteristic curve (AUROC) as the primary performance metric. The AUROC measures the ability of the model to distinguish between classes, in this case, accurately identifying individuals with or without the condition under study. A higher AUROC value, closer to 1, indicates better performance, signifying that the model has a higher probability of correctly classifying the outcomes. We also calculated precision, recall, sensitivity, specificity, balanced accuracy, and the area under the precision-recall curve.

Table 1. Matched Sample Description and Demographics

Sample	Participants	Scanners	Age, Years	Sex, Female/Male
Matched HC				
Alzheimer's Disease	116	13	71.72 (7.12)	55%/45%
ASD	317	25	15.96 (7.45)	17%/83%
Bipolar Disorder	238	3	33.06 (10.50)	55%/45%
Mild Cognitive Impairment	122	3	65.62 (9.91)	42%/58%
Schizophrenia	195	3	30.13 (8.15)	41%/59%
Clinical				
Alzheimer's Disease	116	13	73.11 (7.60)	55%/45%
ASD	317	25	12.35 (4.42)	17%/83%
Bipolar Disorder	238	3	31.61 (11.40)	55%/45%
Mild Cognitive Impairment	122	3	67.25 (9.27)	42%/58%
Schizophrenia	195	3	28.29 (9.45)	41%/59%

Values are presented as *n*, mean (SD), or %.
ASD, autism spectrum disorder; HC, healthy control participant.

Permutation Testing

We used permutation testing to assess whether the AUROCs achieved by our model were different from chance-level performance. To achieve this, we shuffled the diagnosis labels randomly 1000 times for each permutation calculating an AUROC. For significance testing, the original AUROC was compared with the distribution of permuted AUROC values. If

Figure 1. Overview of predicting mental and neurological illnesses. **(A)** The study included 5 clinical datasets: Alzheimer's disease, autism spectrum disorder, bipolar disorder, mild cognitive impairment, and schizophrenia. The input data, together with the samples, consist of both lobular and voxelwise data. **(B)** Individuals without a diagnosis were divided into training and test sets to evaluate the cerebellar normative models. The deviation score (*z* score) measures how much an individual deviates from the norm represented by the estimated population model. **(C)** The analysis utilized the deviation scores derived from the cerebellar lobular and voxelwise normative models. Lobular *z* scores consist of 28 lobular volumes. For voxelwise, deviation scores overlaid onto existing cerebellar atlases including anatomical, task-based, hierarchical, and resting-state parcellations. This process calculated median, variance, and percentage of extreme positive and negative deviation for each atlas' regions of interest (ROIs). Logistic regression was used for each atlas to assess the predictive value of features across all ROIs.

the original AUROC fell within the extreme ends of the permutation distribution ($p < .05$), it was considered statistically significant. We applied an identical approach for the lobular volume features. The comparison between models utilized an approach similar to that outlined in Figures S3 and S4, wherein the previously calculated shuffled AUROC values were used. We calculated the difference in true AUROC scores, as well as the AUROC differences from 1000 permuted datasets, between the 2 models. Subsequently, we compared the true score and the permuted scores to assess statistical significance.

Feature Importance Ranking

We assessed feature importance based on LR coefficients to highlight their influence on the predictions. The coefficients from the model directly infer the relative importance of each feature, thus facilitating interpretation. The standardized magnitude of the coefficient indicates the strength of the effect that a feature has on the prediction, while the sign (positive or negative) indicates the direction of the effect.

RESULTS

We conducted a comprehensive analysis at the lobular and voxelwise level using a variety of models (Figure 1C). The voxelwise model calculations included variance, median, and percentage of deviations across 143,000 voxels, which were organized into 28 ROIs for the anatomical atlas, 10 ROIs for the task-based atlas, 32 ROIs for the hierarchical atlas, and 17 ROIs for the resting-state atlas.

Permutation testing revealed significant predictions for ASD and SZ (AUROC values ranging from 0.56 to 0.65), using various models based on deviations from the cerebellar normative model (Figure 2 and Table S4). Prediction performance for MCI, AD, and BD were not above chance levels. For SZ, the most predictive models were those centered around median and variance measures summarized within ROIs for the voxelwise models. In contrast, for ASD, models based on the lobular volumes and voxelwise variance within ROIs were found to be the most predictive. We explored 2 machine learning approaches, LR and RF, and observed no notable differences between models in terms of feature importance or performance (Figures S3 and S4). This

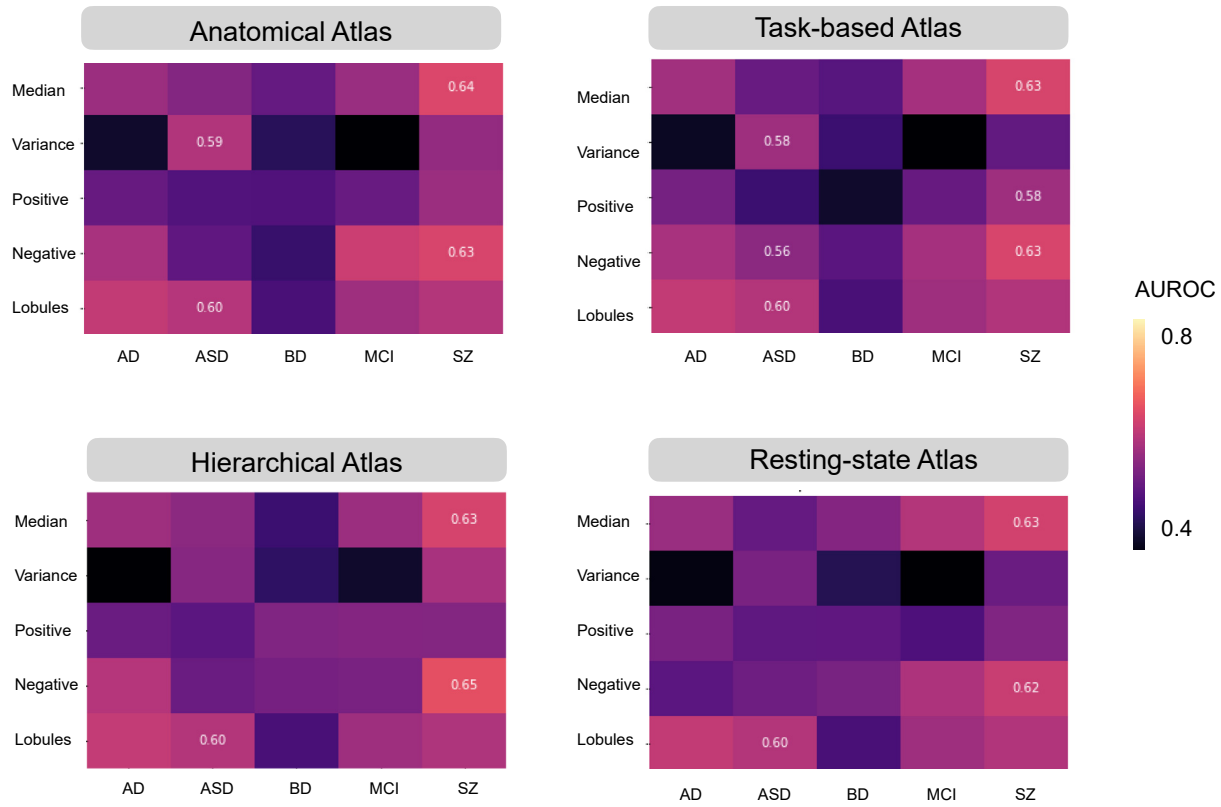

Figure 2. Cerebellar features moderately predict autism spectrum disorder (ASD) and schizophrenia (SZ). **(A)** Information from the anatomical (28 regions), task-based (10 regions), hierarchical (32 regions), or resting-state (17 regions) atlases are compiled into features that were used as predictors by the logistic regression model to make predictions. The area under the receiver operating characteristic curve (AUROC) serves as an important measure in evaluating the performance of a binary classifier, representing a trade-off between the classifier's sensitivity (true positive rate) and specificity (true negative rate). The reliability and robustness of the AUROC were assessed by computing them over 1000 permutations, which aids in determining whether the classifier's performance is statistically significant or due to random chance. **(B–D)** The values that survived multiple comparison are shown. AD, Alzheimer's disease; BD, bipolar disorder; MCI, mild cognitive impairment.

indicates that despite using different methods and parcellation schemes, the core predictions remained robust, affirming the stability and reliability of our modeling approach. We report the linear and interpretable method in terms of features weighs in the main text.

Figure 3 presents the standardized feature importance weights in an LR model used to analyze SZ and ASD (see Figure S2 for all feature importance). For each analysis of lobules or atlases, we report the 2 highest-ranking features. In SZ, significant negative deviation percentages were found in the vermis IX and left IV regions in the anatomical atlas. In task-based functional areas, regions associated with verbal fluency, word comprehension, and mental arithmetic (region 9) and autobiographical recall, visual letter recognition, and

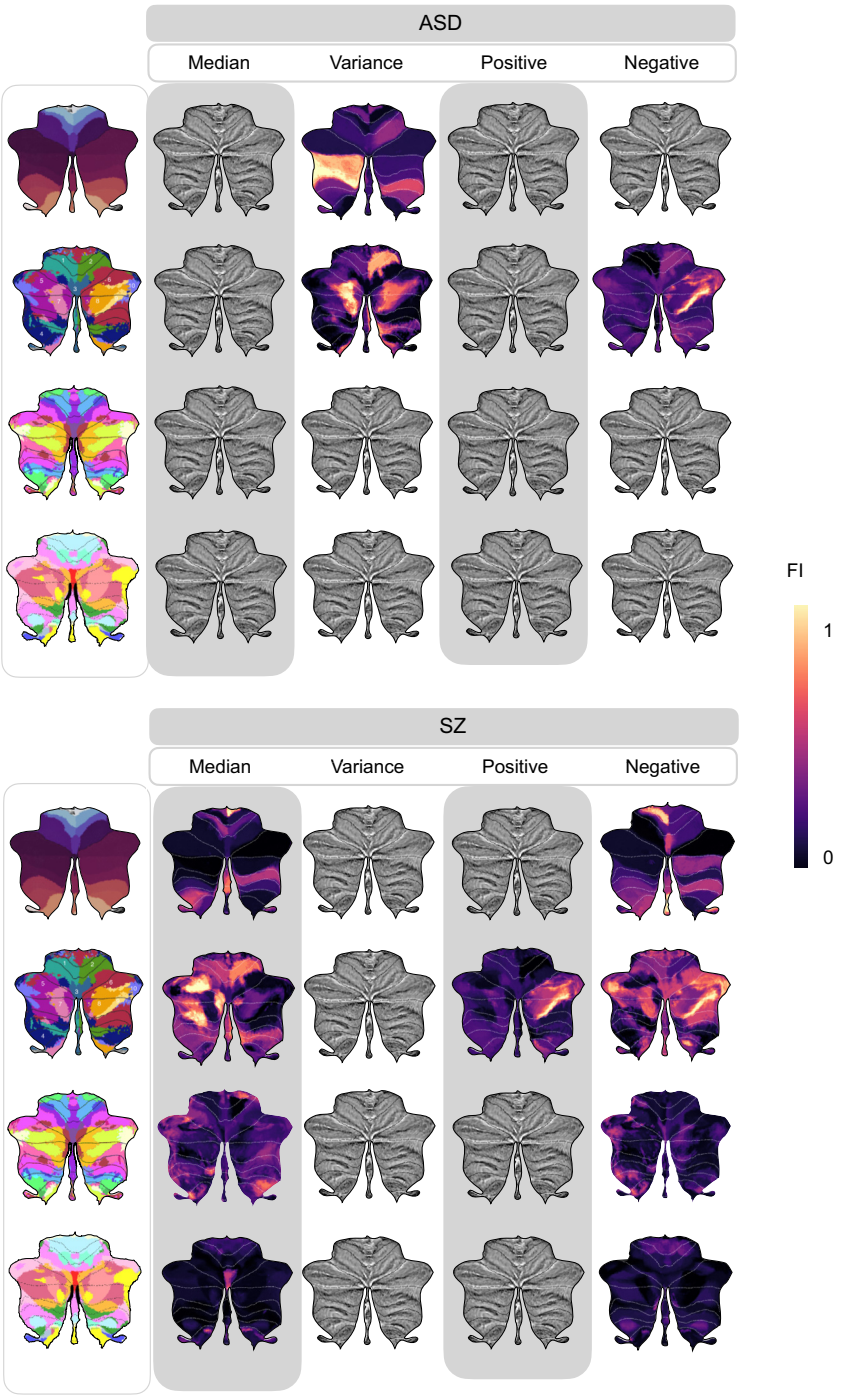

Figure 3. Different regions show distinct feature importance (FI) across atlases in autism spectrum disorder (ASD) and schizophrenia (SZ). The FI values derived from logistic regression reveal the contribution of each specific cerebellar region to predictive modeling relative to average prediction outcomes. FI values accentuate distinct cerebellar regions with unique predictive capabilities as identified in lobules, anatomical, task-based, hierarchical, and resting-state atlases through voxelwise analysis. Features that remained significant after adjustments for multiple comparisons of the area under the receiver operating characteristic curve are shown.

interference resolution (region 10) were notable. The 2 highest-ranking feature importance in the hierarchical atlas were found in the left S1 (social-linguistic-spatial) and left D1 (demand) regions. From the resting-state atlas, limbic A (region 10) and somatomotor A (region 3) emerged as important. For the median in SZ, the anatomical regions right I–III and vermis VIII were highlighted. Using task-based atlases, the top predictive regions were functionally linked to divided attention (region 5) and right-hand movement (region 2). In the hierarchical atlas, the median values were observed in the same regions as the percentage of extreme negative deviations. Predictive models using an atlas based on resting-state atlas highlighted visual B (region 2) and limbic A (region 10).

In ASD, predictive models based on regional variance revealed the 2 highest-ranking feature importance from posterior cerebellar regions of left VIIB and left crus II in the anatomical atlas, while models based on lobular volume features point to right VI and left crus II. Using the task-based functional atlas, the most predictive regions were functionally linked to narrative, emotion, and language processing (region 7) and right-hand movement, motor planning, and divided attention (region 2). Complementary insights and detailed rankings of feature importance are available in Tables S5 to S9.

DISCUSSION

In this study, we aimed to test the predictive power of deviations from normal cerebellar anatomy with respect to classifying mental and neurological disorders and yielded 2 main findings. First, we demonstrated that cerebellar features offered moderate power for prediction of ASD and SZ but did not reliably distinguish reference samples from patients with BD, MCI, or AD. Second, feature importance analyses showed that both anterior and posterior regions of the cerebellum were dominant features of ASD and SZ.

Our study reveals that features derived from lobular and voxelwise normative models possess moderate predictive capabilities in ASD and SZ. This is consistent with our previous study, which revealed small to medium case-control differences in normative cerebellar anatomy for both ASD and SZ (15). On the other hand, as functional topography does not consistently adhere to anatomical boundaries in the cerebellum, we also examined task-based, hierarchical, and resting-state atlases in voxelwise normative space. As a result, no single atlas consistently emerged as superior to the others. However, we believe that using various atlases aids in the interpretation of our findings.

A comprehensive feature importance analysis for predicting SZ highlighted significant contributions from regions associated with both motor (56,57) and cognitive (20) functions. Within the anatomical atlas superimposed on the voxelwise cerebellar maps, vermis IX and left IV exhibited the 2 highest-ranking feature importance for percentage of extreme negative deviations, while right I–III and vermis VIII were most prominent in median values. Median features, which reflect the central tendency across *z* scores within one region, largely overlapped with those identified in the analysis of extreme negative deviations, which measure divergence from normative values. Notably, vermis IX has consistently been reported to exhibit reductions in individuals with SZ, underscoring its potential role in the disorder's pathology (58–61). These findings are consistent with previous research suggesting that the limbic vermis plays a crucial role in emotional processing, facial expression recognition (62–64), and mentalizing—the ability to understand others' mental states (22,64–66). Recent studies (67) have also highlighted cerebellar hypoplasia, primarily affecting the posterior vermis, in individuals with SZ or undifferentiated psychosis. Additionally, the anterior cerebellum, including lobules I–IV, has established connections with the primary motor cortex, which is critical for motor function (68). This connection may explain the motor dysfunctions in SZ, such as impairments in eye-blink conditioning, timing, postural control, and motor learning, which are associated with reduced volumes in anterior cerebellar regions and the vermis (69–71). The involvement of both motor and cognitive regions underscores the disorder's complexity, providing deeper insights into its diverse facets.

When the voxelwise cerebellar maps were mapped onto a task-based atlas for extreme negative deviations (23), regions linked to verbal fluency and autobiographical recall were identified, while divided attention and right-hand movement were associated with median deviations in SZ. In a hierarchical atlas, models of extreme negative deviation and median feature importance were predominantly highlighted in the left S1 (social-linguistic-spatial) and left D1 (demand) regions, which emphasize linguistic processing and verb generation. A recent study (18) linked language difficulties in early psychosis to alterations in the right posterolateral cerebellar region, an area involved in verb generation and cognitive functions such as attention and memory (23). This suggests that individuals with early psychosis may struggle with verbal expression and thought control, impairing perceptual processing. These regions overlap with those previously associated with speech perception and production (72).

Mapped to the resting-state atlas, the most significant features included limbic A and somatomotor A in terms of extreme negative deviations, while visual B and limbic A were notable for median values. The limbic network is involved in emotion processing, memory, and behavior, while the somatomotor network governs motor processing and execution, and the visual network processes visual information. SZ is often accompanied by oculomotor abnormalities, affecting eye movement control in response to visual stimuli and anticipated actions (73). Studies of cerebro-cerebellar connectivity have reported increased connectivity within somatomotor, sensorimotor, and default mode networks but decreased connectivity in higher-order networks, including attention, salience, and executive control regions (74,75). While direct comparisons between functional connectivity studies and structural analyses may be challenging due to methodological differences, these findings remain relevant.

Previous studies have reported inconsistent and hard-to-replicate findings on the relationship between cerebellar volume and ASD (15,76). Interestingly, ASD was best predicted by the variance of *z* scores within individual parcellations of the cerebellum, indicating greater voxel-level variability in different regions. Feature importance analyses in ASD highlighted left VIIB and left crus II in the anatomical atlas, as well as narrative, emotion, and language processing regions and right-hand movement in the task-based atlas. Crus I–II and lobule VIIB

are densely connected to prefrontal and parietal cortices through cerebello-thalamo-cortico-pontine circuits (77) that are critical for higher-level processes. Its substantial heterogeneity, ranging from high-functioning individuals to individuals who require significant support, presents challenges in identifying a common neurobiological basis (78).

Prior research has consistently demonstrated strong classification of dementia using whole-brain imaging data, with AUROC values ranging from 0.904 to 0.920 (3). Thus, the absence of significant predictive models for BD, MCI, and AD was unexpected, although it is worth noting that the effects of MCI and AD were relatively small in our previous study as well (15). While null findings should be interpreted with caution, the lack of effects in a moderately large sample of baseline patients with AD suggests that the cerebellum may be relatively spared (79,80). However, both typical aging and AD are associated with gray matter loss in the cerebellum, particularly in crus I–II and lobule VI. In typical aging, this decline occurs bilaterally, whereas in AD, it is more pronounced in the right hemisphere (81). Given the growing research on cerebellar aging (82), additional studies are needed to determine how MCI and AD pathology contribute to cerebellar atrophy and to what extent the cerebellum remains relatively preserved. Similarly, research on BD and its cerebellar involvement is hindered by inconsistent findings (83), underscoring the need for more comprehensive investigations.

There are limitations to consider in our study. First, harmonizing behavioral, cognitive, genetic, phenotypic, lifestyle, symptomatology, and medical history data across various datasets poses significant challenges, especially when aiming for a large sample size essential for assessing generalizability. The limited predictive power of the trained machine learning models (84) should be taken into consideration when interpreting the current findings. In multivariate models, feature importance must be assessed with regard to the overall model context. Collinearity among features can result in fluctuations in their rankings, necessitating cautious interpretation. For practicality, we have concentrated our discussion on the 2 features that emerged as highest in ranking. Next, accurately classifying complex clinical conditions is challenging due to the intrinsic heterogeneity of these conditions, which manifests as a wide array of symptoms and genetic variations. Some individuals may exhibit resilience due to genetic or lifestyle factors, which can complicate accurate predictions (85). The key challenge in normative modeling lies in interpreting deviations at the individual level. The central question is whether these deviations are biologically significant or merely artifacts resulting from signal dropout during imaging. Therefore, individual-level interpretation is still an area under active development. Furthermore, the existence of subgroups within heterogeneous conditions, such as ASD, complicates the interpretation of performance metrics of prediction models. Neurodevelopmental changes raise concerns about the appropriateness of applying adult template space and atlases to younger children and adolescents (86). Including other key brain regions and utilizing a multimodal approach that integrates different types of brain imaging data may improve predictions (87,88). Future studies should compare cerebellar and whole-brain models to clarify the cerebellum's unique contribution within the broader neural context. Given the large sample size, we manually inspected about 5% of the scans to maintain quality control. Nevertheless, we acknowledge the limitations in accurately depicting different atlases with varying border including lobular segmentation. The cerebellum's distinct position within the skull and its intricate folding pattern also present challenges in obtaining precise MRI data. Because we incorporated a large number of samples, the normative models are not affected by occasional outliers that might have been missed in our extensive quality control procedures, which additionally strengthens our confidence in the robustness of the reported findings. Finally, an AUROC value in the range of 0.7 to 0.8 can be deemed acceptable for certain clinical applications (89), indicating fair discrimination that includes the range of our model. However, for many clinical scenarios, this may not suffice, as values from 0.8 to 0.9 are generally regarded as appropriate (90). Future research efforts should aim to address these limitations and further enhance our understanding of predictive models.

Conclusions

In this study, we tested the value of cerebellar-derived features for predictions of 5 mental and neurological conditions. The analysis revealed moderate prediction performance for ASD and SZ, with strongest contributions across cerebellar regions aided by 4 cerebellar atlases that enhanced the interpretability of the findings.

ACKNOWLEDGMENTS AND DISCLOSURES

The work was supported by the South-Eastern Norway Regional Health Authority (Grant Nos. 2021040 [to MK and TM]; 2018037, 2018076, 2019101, 2021070, 2023012, 500189), Deutsche Forschungsgemeinschaft Emmy Noether (Grant No. 513851350 [to TW]), NordForsk (Grant No. 164218), the Research Council of Norway (Grant Nos. 249795, 248238, 276082, 286838, 288083, 323951, 324499), Stiftelsen Kristian Gerhard Jebsen, ERA-Net Cofund through the ERA PerMed project IMPLEMENT, and the European Research Council (ERC) under the European Union's Horizon 2020 Research and Innovation Program (ERC Starting Grant No. 802998). AFM gratefully acknowledges funding from the ERC (MENTAL-PRECISION Grant No. 101001118) and from the Raynor Foundation. The funders had no role in conception of the study or the analyses and/or interpretations of the results. Data collection and sharing for this project was funded by the ADNI (National Institutes of Health Grant No. U01 AG024904) and Department of Defense ADNI (Award No. W81XWH-12-2-0012).

ADNI is funded by the National Institute on Aging and the National Institute of Biomedical Imaging and Bioengineering and through generous contributions from the following: AbbVie, Alzheimer's Association; Alzheimer's Drug Discovery Foundation; Araclon Biotech; BioClinica, Inc.; Biogen; Bristol-Myers Squibb Company; CereSpir, Inc.; Cogstate; Eisai Inc.; Elan Pharmaceuticals, Inc.; Eli Lilly and Company; EuroImmun; F. Hoffmann-La Roche Ltd. and its affiliated company Genentech, Inc.; Fujirebio; GE Healthcare; IXICO Ltd.; Janssen Alzheimer Immunotherapy Research & Development, LLC; Johnson & Johnson Pharmaceutical Research & Development LLC; Lumosity; Lundbeck; Merck & Co., Inc.; Meso Scale Diagnostics, LLC; NeuroRx Research; Neurotrack Technologies; Novartis Pharmaceuticals Corporation; Pfizer Inc.; Piramal Imaging; Servier; Takeda Pharmaceutical Company; and Transition Therapeutics. The Canadian Institutes of Health Research is providing funds to support ADNI clinical sites in Canada. Private sector contributions are facilitated by the Foundation for the National Institutes of Health (www.fnih.org). The grantee organization is the Northern California Institute for Research and Education, and the study is coordinated by the Alzheimer's Therapeutic Research Institute at the University of Southern California.

TM, TW, and MK originally conceived the project. MK, NS, TW, TM, and EHL performed the analyses. MK, TW, and TM wrote the initial draft of the

article. OAA, GR, KP, DA, GS, NES, OBS, AFM, CFB, TU, TW, and LTW contributed to data curation. All authors discussed the results and contributed to the final version of the article.

We thank all the individuals who participated in the studies and acknowledge the contributions of the clinicians and researchers who were involved in the recruitment and assessment of participants for making this work possible. We performed this work on the Services for sensitive data, University of Oslo, Norway, with resources provided by UNINETT Sigma2-the National Infrastructure for High-Performance Computing and Data Storage in Norway.

Data used in preparation of this article were obtained from the ADNI database (adni.loni.usc.edu). As such, the investigators within the ADNI contributed to the design and implementation of ADNI and/or provided data but did not participate in analysis or the writing of this report. A complete listing of ADNI investigators can be found at https://adni.loni.usc.edu/help-faqs/adni-documentation/ within ADNI Acknowledgment List for ADNI Publication.

In this study, we used brain imaging from ABIDE, ADNI, AIBL, DEMGEN, and TOP. The cerebellar normative models from this work are available on via PCNportal (91): https://pcnportal.dccn.nl/. These are analyses of publicly and privately available data. Description of informed consent and other ethical procedures is extensively described in each study, referenced in the article. The data were stored and analyzed using University of Oslo's secure platform, Services for sensitive data, in compliance with Norwegian privacy regulations. All code used in this work is available at FreeSurfer (https://surfer.nmr.mgh.harvard.edu), FSL (https://fsl.fmrib.ox.ac.uk/fsl/fslwiki/FslInstallation), ACAPULCO (https://gitlab.com/shuohan/acapulco), and SUIT (https://github.com/jdiedrichsen/suit). Code for the normative model is available as an open-source python package, the PCN toolkit (https://github.com/amarquand/PCNtoolkit). Additional code is forked to or published on https://github.com/MHM-lab. ADNI data are disseminated by the Laboratory for Neuro Imaging at the University of Southern California. Also, data used in preparation of this article were obtained from the AIBL databases (adni.loni.usc.edu).

A previous version of this article was published as a preprint on medRxiv: https://www.medrxiv.org/content/10.1101/2024.12.10.24318590v1.

OAA has received speaker fees from Lundbeck, Janssen, Otsuka, and Sunovion and is a consultant to Cortechs.ai and Precision-Health.ai. EHL has received speaker fees from Lundbeck and is the CTO and shareholder of baba.vision. LTW and TW are shareholders of baba.vision. KP contributed to clinical trials for Roche (clinical trial ID: BN29553) and Novo Nordisk (clinical trial ID: NN6535-4730), outside the submitted work. All other authors report no biomedical financial interests or potential conflicts of interest.

ARTICLE INFORMATION

From the Centre for Precision Psychiatry, Division of Mental Health and Addiction, University of Oslo and Oslo University Hospital, Oslo, Norway (MK, EHL, NES, OBS, GR, DA, OAA, LTW, TW, TM); Department of Psychology, University of Oslo, Oslo, Norway (MK, EHL, TU, DA, LTW); Department of Psychiatry and Psychotherapy, University of Tübingen, Tübingen, Germany (NS, TW); German Center for Mental Health, Tübingen, Germany (NS, TW); Department of Cognitive Neuroscience, Radboud University Medical Centre, Nijmegen, the Netherlands (SR); Donders Institute, Radboud University, Nijmegen, the Netherlands (SR, CFB, AFM); Department of Psychiatry, University of Michigan, Ann Arbor, Michigan (SR); Department of Geriatric Medicine, Oslo University Hospital, Oslo, Norway (GS, KP); The Norwegian National Centre for Ageing and Health, Vestfold Hospital Trust, Tønsberg, Norway (GS, KP); Institute for Clinical Medicine, University of Oslo, Oslo, Norway (GS); Section for Clinical Psychosis Research, Division of Mental Health and Addiction, Oslo University Hospital, Oslo, Norway (NES, TU); Division of Mental Health and Substance Abuse, Diakonhjemmet Hospital, Oslo, Norway (NES); Otto Hahn Research Group for Cognitive Neurogenetics, Max Planck Institute for Human Cognitive and Brain Sciences, Leipzig, Germany (AM, SLV); Institute of Neurosciences and Medicine (INM-7), Research Centre Jülich, Jülich, Germany (SLV); Institute of Systems Neuroscience, Heinrich-Heine-Universität Düsseldorf, Düsseldorf, Germany (SLV); Centre for Functional MRI of the Brain, Nuffield Department of Clinical Neurosciences, Wellcome Centre for Integrative Neuroimaging, University of Oxford, Oxford, United Kingdom (CFB); Department of Neuroimaging, Center of Neuroimaging Sciences, Institute of Psychiatry, King's College London, London, United Kingdom (AFM); KG Jebsen Centre for Neurodevelopmental Disorders, University of Oslo, Oslo, Norway (OAA, LTW); Department of Behavioral Science, School of Health Sciences, Oslo Metropolitan University, Oslo, Norway (TM); and Department of Psychology, Pedagogy and Law, School of Health Sciences, Kristiania University College, Oslo, Norway (TM).

TW and TM contributed equally to this work.

Address correspondence to Milin Kim, M.Phil., at milink@student.sv.uio.no.

Received Jan 9, 2025; revised May 16, 2025; accepted May 21, 2025.

Supplementary material cited in this article is available online at https://doi.org/10.1016/j.bpsgos.2025.100541.

REFERENCES

1. Chen J, Patil KR, Yeo BTT, Eickhoff SB (2023): Leveraging machine learning for gaining neurobiological and nosological insights in psychiatric research. Biol Psychiatry 93:18–28.
2. Meehan AJ, Lewis SJ, Fazel S, Fusar-Poli P, Steyerberg EW, Stahl D, Danese A (2022): Clinical prediction models in psychiatry: A systematic review of two decades of progress and challenges. Mol Psychiatry 27:2700–2708.
3. Leonardsen EH, Persson K, Grødem E, Dinsdale N, Schellhorn T, Roe JM, *et al.* (2024): Constructing personalized characterizations of structural brain aberrations in patients with dementia using explainable artificial intelligence. Npj Digit Med 7:110.
4. Rashid B, Calhoun V (2020): Towards a brain-based predictome of mental illness. Hum Brain Mapp 41:3468–3535.
5. Wolfers T, Buitelaar JK, Beckmann CF, Franke B, Marquand AF (2015): From estimating activation locality to predicting disorder: A review of pattern recognition for neuroimaging-based psychiatric diagnostics. Neurosci Biobehav Rev 57:328–349.
6. Zhu Y, Maikusa N, Radua J, Sämann PG, Fusar-Poli P, Agartz I, *et al.* (2024): Using brain structural neuroimaging measures to predict psychosis onset for individuals at clinical high-risk. Mol Psychiatry 29:1465–1477.
7. Parvizi J (2009): Corticocentric myopia: Old bias in new cognitive sciences. Trends Cogn Sci 13:354–359.
8. Moussa-Tooks AB, Rogers BP, Huang AS, Sheffield JM, Heckers S, Woodward ND (2022): Cerebellar structure and cognitive ability in psychosis. Biol Psychiatry 92:385–395.
9. Hughes DE, Kunitoki K, Elyounssi S, Luo M, Bazer OM, Hopkinson CE, *et al.* (2023): Genetic patterning for child psychopathology is distinct from that for adults and implicates fetal cerebellar development. Nat Neurosci 26:959–969.
10. Schmahmann JD (2016): Cerebellum in Alzheimer's disease and frontotemporal dementia: Not a silent bystander. Brain 139:1314–1318.
11. Moberget T, Doan NT, Alnæs D, Kaufmann T, Córdova-Palomera A, Lagerberg TV, *et al.* (2018): Cerebellar volume and cerebellocerebral structural covariance in schizophrenia: A multisite mega-analysis of 983 patients and 1349 healthy controls. Mol Psychiatry 23:1512–1520.
12. D'Mello AM, Stoodley CJ (2015): Cerebro-cerebellar circuits in autism spectrum disorder. Front Neurosci 9:408.
13. Stoodley CJ (2016): The cerebellum and neurodevelopmental disorders. Cerebellum 15:34–37.
14. van der Heijden ME, Gill JS, Sillitoe RV (2021): Abnormal cerebellar development in autism spectrum disorders. Dev Neurosci 43:181–190.
15. Kim M, Leonardsen E, Rutherford S, Selbæk G, Persson K, Steen NE, *et al.* (2024): Mapping cerebellar anatomical heterogeneity in mental and neurological illnesses. Nat Mental Health 2:1196–1207.
16. Laidi C, d'Albis MA, Wessa M, Linke J, Phillips ML, Delavest M, *et al.* (2015): Cerebellar volume in schizophrenia and bipolar I disorder with and without psychotic features. Acta Psychiatr Scand 131:223–233.
17. American Psychiatric Association (2013): Diagnostic and Statistical Manual of Mental Disorders, 5th ed. Washington, DC: American Psychiatric Association.
18. Toyota E, Mackinley M, Silva AM, Jiang Y, Dalal TC, Nettekoven C, Palaniyappan L (2025): Cerebellum as a neural substrate for impoverishment in early psychosis. Neuropsychologia 210:109094.

19. Schmahmann JD (2004): Disorders of the cerebellum: Ataxia, dysmetria of thought, and the cerebellar cognitive affective syndrome. J Neuropsychiatry Clin Neurosci 16:367–378.
20. Schmahmann JD (2019): The cerebellum and cognition. Neurosci Lett 688:62–75.
21. Schmahmann JD (2021): Emotional disorders and the cerebellum: Neurobiological substrates, neuropsychiatry, and therapeutic implications. Handb Clin Neurol 183:109–154.
22. Buckner RL, Krienen FM, Castellanos A, Diaz JC, Yeo BTT (2011): The organization of the human cerebellum estimated by intrinsic functional connectivity. J Neurophysiol 106:2322–2345.
23. King M, Hernandez-Castillo CR, Poldrack RA, Ivry RB, Diedrichsen J (2019): Functional boundaries in the human cerebellum revealed by a multi-domain task battery. Nat Neurosci 22:1371–1378.
24. Ho DE, Imai K, King G, Stuart EA (2011): MatchIt: Nonparametric preprocessing for parametric causal inference. J Stat Soft 42:1–28.
25. Ségonne F, Dale AM, Busa E, Glessner M, Salat D, Hahn HK, Fischl B (2004): A hybrid approach to the skull stripping problem in MRI. Neuroimage 22:1060–1075.
26. Jenkinson M, Beckmann CF, Behrens TEJ, Woolrich MW, Smith SM (2012): FSL. Neuroimage 62:782–790.
27. Jenkinson M, Smith S (2001): A global optimisation method for robust affine registration of brain images. Med Image Anal 5:143–156.
28. Han S, An Y, Carass A, Prince JL, Resnick SM (2020): Longitudinal analysis of regional cerebellum volumes during normal aging. Neuroimage 220:117062.
29. Tustison NJ, Avants BB, Cook PA, Zheng Y, Egan A, Yushkevich PA, Gee JC (2010): N4ITK: Improved N3 bias correction. IEEE Trans Med Imaging 29:1310–1320.
30. Fonov V, Evans AC, Botteron K, Almli CR, McKinstry RC, Collins DL, Brain Development Cooperative Group (2011): Unbiased average age-appropriate atlases for pediatric studies. Neuroimage 54:313–327.
31. Carass A, Cuzzocreo JL, Han S, Hernandez-Castillo CR, Rasser PE, Ganz M, *et al.* (2018): Comparing fully automated state-of-the-art cerebellum parcellation from magnetic resonance images. Neuroimage 183:150–172.
32. Kerestes R, Han S, Balachander S, Hernandez-Castillo C, Prince JL, Diedrichsen J, Harding IH (2022): A standardized pipeline for examining human cerebellar grey matter morphometry using structural magnetic resonance imaging. J Vis Exp 180.
33. Diedrichsen J (2006): A spatially unbiased atlas template of the human cerebellum. NeuroImage 33:127–138.
34. Diedrichsen J, Balsters JH, Flavell J, Cussans E, Ramnani N (2009): A probabilistic MR atlas of the human cerebellum. NeuroImage 46:39–46.
35. Marquand AF, Rezek I, Buitelaar J, Beckmann CF (2016): Understanding heterogeneity in clinical cohorts using normative models: Beyond case-control studies. Biol Psychiatry 80:552–561.
36. Marquand AF, Kia SM, Zabihi M, Wolfers T, Buitelaar JK, Beckmann CF (2019): Conceptualizing mental disorders as deviations from normative functioning. Mol Psychiatry 24:1415–1424.
37. Rutherford S, Kia SM, Wolfers T, Fraza C, Zabihi M, Dinga R, *et al.* (2022): The normative modeling framework for computational psychiatry. Nat Protoc 17:1711–1734.
38. Rutherford S, Barkema P, Tso IF, Sripada C, Beckmann CF, Ruhe HG, Marquand AF (2023): Evidence for embracing normative modeling. eLife 12:e85082.
39. Floris DL, Wolfers T, Zabihi M, Holz NE, Zwiers MP, Charman T, *et al.* (2020): Atypical Brain Asymmetry in autism – A candidate for clinically meaningful stratification. Biol Psychiatry Cogn Neurosci Neuroimaging 6:802–812.
40. Remiszewski N, Bryant JE, Rutherford SE, Marquand AF, Nelson E, Askar I, *et al.* (2022): Contrasting case-control and normative reference approaches to capture clinically relevant structural brain abnormalities in patients with first-episode psychosis who are antipsychotic naive. JAMA Psychiatry 79:1133–1138.
41. Verdi S, Kia SM, Yong KXX, Tosun D, Schott JM, Marquand AF, Cole JH (2023): Revealing individual neuroanatomical heterogeneity in Alzheimer disease using neuroanatomical normative modeling. Neurology 100:e2442–e2453.
42. Wolfers T, Doan NT, Kaufmann T, Alnæs D, Moberget T, Agartz I, *et al.* (2018): Mapping the heterogeneous phenotype of schizophrenia and bipolar disorder using normative models. JAMA Psychiatry 75:1146–1155.
43. Wolfers T, Beckmann CF, Hoogman M, Buitelaar JK, Franke B, Marquand AF (2020): Individual differences v. the average patient: Mapping the heterogeneity in ADHD using normative models. Psychol Med 50:314–323.
44. Rios G, Tobar F (2019): Compositionally-warped Gaussian processes. Neural Netw 118:235–246.
45. Fraza CJ, Dinga R, Beckmann CF, Marquand AF (2021): Warped Bayesian linear regression for normative modelling of big data. Neuroimage 245:118715.
46. Dinga R, Fraza CJ, Bayer JMM, Kia SM, Beckmann CF, Marquand AF (2021): Normative modeling of neuroimaging data using generalized additive models of location scale and shape. bioRxiv https://doi.org/10.1101/2021.06.14.448106.
47. Kia SM, Huijsdens H, Rutherford S, Dinga R, Wolfers T, Mennes M, *et al.* (2021): Federated multi-site normative modeling using hierarchical Bayesian regression. bioRxiv https://doi.org/10.1101/2021.05.28.446120.
48. Bayer JMM, Dinga R, Kia SM, Kottaram AR, Wolfers T, Lv J, *et al.* (2022): Accommodating site variation in neuroimaging data using normative and hierarchical Bayesian models. Neuroimage 264:119699.
49. Nettekoven C, Zhi D, Shahshahani L, Pinho AL, Saadon-Grosman N, Buckner RL, Diedrichsen J (2024): A hierarchical atlas of the human cerebellum for functional precision mapping. bioRxiv https://doi.org/10.1101/2023.09.14.557689.
50. Yeo BTT, Krienen FM, Sepulcre J, Sabuncu MR, Lashkari D, Hollinshead M, *et al.* (2011): The organization of the human cerebral cortex estimated by intrinsic functional connectivity. J Neurophysiol 106:1125–1165.
51. Alnæs D, Kaufmann T, van der Meer D, Córdova-Palomera A, Rokicki J, Moberget T, *et al.* (2019): Brain heterogeneity in schizophrenia and its association with polygenic risk. JAMA Psychiatry 76:739–748.
52. Brugger SP, Howes OD (2017): Heterogeneity and homogeneity of regional brain structure in schizophrenia: A meta-analysis. JAMA Psychiatry 74:1104–1111.
53. Zabihi M, Oldehinkel M, Wolfers T, Frouin V, Goyard D, Loth E, *et al.* (2019): Dissecting the heterogeneous cortical anatomy of autism spectrum disorder using normative models. Biol Psychiatry Cogn Neurosci Neuroimaging 4:567–578.
54. Pedregosa F, Varoquaux G, Gramfort A, Michel V, Thirion B, Grisel O, *et al.* (2018): Scikit-learn: machine learning in Python. arXiv https://doi.org/10.48550/arXiv.1201.0490.
55. Chen T, Guestrin C (2016): XGBoost: A scalable tree boosting system. arXiv https://doi.org/10.48550/arXiv.1603.02754.
56. Walther S (2015): Psychomotor symptoms of schizophrenia map on the cerebral motor circuit. Psychiatry Res 233:293–298.
57. Walther S, Strik W (2012): Motor symptoms and schizophrenia. Neuropsychobiology 66:77–92.
58. Heath RG, Franklin DE, Walker CF, Keating JW (1982): Cerebellar vermal atrophy in psychiatric patients. Biol Psychiatry 17:569–583.
59. Jacobsen LK, Giedd JN, Berquin PC, Krain AL, Hamburger SD, Kumra S, Rapoport JL (1997): Quantitative morphology of the cerebellum and fourth ventricle in childhood-onset schizophrenia. Am J Psychiatry 154:1663–1669.
60. Picard H, Amado I, Mouchet-Mages S, Olié J-P, Krebs M-O (2008): The role of the cerebellum in schizophrenia: An update of clinical, cognitive, and functional evidences. Schizophr Bull 34:155–172.
61. Andreasen NC, Pierson R (2008): The role of the cerebellum in schizophrenia. Biol Psychiatry 64:81–88.
62. Brady RO, Gonsalvez I, Lee I, Öngür D, Seidman LJ, Schmahmann JD, *et al.* (2019): Cerebellar-prefrontal network connectivity and negative symptoms in schizophrenia. Am J Psychiatry 176:512–520.

63. Metoki A, Wang Y, Olson IR (2022): The social cerebellum: A large-scale investigation of functional and structural specificity and connectivity. Cereb Cortex 32:987–1003.
64. Van Overwalle F (2024): Social and emotional learning in the cerebellum. Nat Rev Neurosci 25:776–791.
65. Clausi S, Olivito G, Lupo M, Siciliano L, Bozzali M, Leggio M (2018): The cerebellar predictions for social interactions: Theory of mind abilities in patients with degenerative cerebellar atrophy. Front Cell Neurosci 12:510.
66. Van Overwalle F, Manto M, Cattaneo Z, Clausi S, Ferrari C, Gabrieli JDE, *et al.* (2020): Consensus paper: Cerebellum and social cognition. Cerebellum 19:833–868.
67. Leslie AC, Ward MP, Dobyns WB (2024): Undifferentiated psychosis or schizophrenia associated with vermis-predominant cerebellar hypoplasia. Am J Med Genet A 194:e63416.
68. Bernard JA, Mittal VA (2014): Cerebellar-motor dysfunction in schizophrenia and psychosis-risk: The importance of regional cerebellar analysis approaches. Front Psychiatry 5:160.
69. Edwards CR, Newman S, Bismark A, Skosnik PD, O'Donnell BF, Shekhar A, *et al.* (2008): Cerebellum volume and eyeblink conditioning in schizophrenia. Psychiatry Res 162:185–194.
70. Greenstein D, Lenroot R, Clausen L, Chavez A, Vaituzis AC, Tran L, *et al.* (2011): Cerebellar development in childhood onset schizophrenia and non-psychotic siblings. Psychiatry Res 193:131–137.
71. Ding Y, Ou Y, Pan P, Shan X, Chen J, Liu F, *et al.* (2019): Cerebellar structural and functional abnormalities in first-episode and drug-naive patients with schizophrenia: A meta-analysis. Psychiatry Res Neuroimaging 283:24–33.
72. Skipper JI, Lametti DR (2021): Speech perception under the tent: A domain-general predictive role for the cerebellum. J Cogn Neurosci 33:1517–1534.
73. Hutton S, Kennard C (1998): Oculomotor abnormalities in schizophrenia: A critical review. Neurology 50:604–609.
74. Shinn AK, Roh YS, Ravichandran CT, Baker JT, Öngür D, Cohen BM (2017): Aberrant cerebellar connectivity in bipolar disorder with psychosis. Biol Psychiatry Cogn Neurosci Neuroimaging 2: 438–448.
75. Ji JL, Diehl C, Schleifer C, Tamminga CA, Keshavan MS, Sweeney JA, *et al.* (2019): Schizophrenia exhibits bi-directional brain-wide alterations in cortico-striato-cerebellar circuits. Cereb Cortex 29:4463–4487.
76. Traut N, Beggiato A, Bourgeron T, Delorme R, Rondi-Reig L, Paradis A-L, Toro R (2018): Cerebellar volume in autism: Literature meta-analysis and analysis of the autism brain imaging data exchange cohort. Biol Psychiatry 83:579–588.
77. Becker EBE, Stoodley CJ (2013): Autism spectrum disorder and the cerebellum. Int Rev Neurobiol 113:1–34.
78. Verhoeff B (2015): Fundamental challenges for autism research: The science–practice gap, demarcating autism and the unsuccessful search for the neurobiological basis of autism. Med Health Care Philos 18:443–447.
79. Bernard JA, Seidler RD (2014): Moving forward: Age effects on the cerebellum underlie cognitive and motor declines. Neurosci Biobehav Rev 42:193–207.
80. Liang KJ, Carlson ES (2020): Resistance, vulnerability and resilience: A review of the cognitive cerebellum in aging and neurodegenerative diseases. Neurobiol Learn Mem 170:106981.
81. Gellersen HM, Guell X, Sami S (2021): Differential vulnerability of the cerebellum in healthy ageing and Alzheimer's disease. Neuroimage Clin 30:102605.
82. Bernard JA, McOwen KM, Huynh AT (2023): New frontiers for the understanding of aging: The power and possibilities of studying the cerebellum. Curr Opin Behav Sci 54:101311.
83. Parker N, Ching CRK (2025): Mapping structural neuroimaging trajectories in bipolar disorder: Neurobiological and clinical implications [published online February 13]. Biol Psychiatry.
84. Arbabshirani MR, Plis S, Sui J, Calhoun VD (2017): Single subject prediction of brain disorders in neuroimaging: Promises and pitfalls. Neuroimage 145:137–165.
85. Venkatraghavan V, Voort SR van der, Bos D, Smits M, Barkhof F, Niessen WJ, *et al.* (2023): Computer-aided diagnosis and prediction in brain disorders. In: Colliot O, editor. Machine Learning for Brain Disorders. New York, NY: Springer, 459–490.
86. Gaiser C, van der Vliet R, de Boer AAA, Donchin O, Berthet P, Devenyi GA, *et al.* (2024): Population-wide cerebellar growth models of children and adolescents. Nat Commun 15:2351.
87. Rokicki J, Wolfers T, Nordhøy W, Tesli N, Quintana DS, Alnaes D, *et al.* (2021): Multimodal imaging improves brain age prediction and reveals distinct abnormalities in patients with psychiatric and neurological disorders. Hum Brain Mapp 42:1714–1726.
88. Tavares V, Vassos E, Marquand A, Stone J, Valli I, Barker GJ, *et al.* (2022): Prediction of transition to psychosis from an at-risk mental state using structural neuroimaging, genetic, and environmental data. Front Psychiatry 13:1086038.
89. Mandrekar JN (2010): Receiver operating characteristic curve in diagnostic test assessment. J Thorac Oncol 5:1315–1316.
90. Zarogianni E, Storkey AJ, Borgwardt S, Smieskova R, Studerus E, Riecher-Rössler A, Lawrie SM (2019): Individualized prediction of psychosis in subjects with an at-risk mental state. Schizophr Res 214:18–23.
91. Barkema P, Rutherford S, Lee H-C, Kia SM, Savage H, Beckmann C, Marquand A (2023): Predictive Clinical Neuroscience Portal (PCNportal): Instant online access to research-grade normative models for clinical neuroscientists. Wellcome Open Res 8:326.